

Simultaneous Heat and Mass Transfer in Packed Bed Catalytic Reactors

K. Kamiuto* and S. Saitoh†
Oita University, Oita 870-11, Japan

Our previous quasihomogeneous model for heat transfer in packed beds is extended so as to include mass transfer in the beds. A porosity-dependent mass dispersion coefficient is incorporated into the previous model. To examine the adequacy of the model, the sulfur dioxide reactor of Schuler et al. is analyzed theoretically utilizing a finite difference scheme. The theoretical results agreed well with the experimental data without introducing any adjustable parameters.

Nomenclature

C = inertial coefficient
 c_p = specific heat
 Da = Darcy number
 Dam = Damköhler number
 D_d = mass dispersion coefficient
 D_e = effective molecular diffusivity of a reactant within a packed bed
 D_m = molecular diffusivity of a reactant in air
 d_p = particle diameter
 E_u = dimensionless pressure gradient
 Fh = Forchheimer number
 H = total heat of reaction
 h_s = local heat transfer coefficient
 K = permeability
 K_0 = equilibrium constant
 K_1 = adsorption equilibrium constant for oxygen
 K_2 = adsorption equilibrium constant for SO_3
 k = specific rate constant
 k_d = thermal dispersion conductivity of a packed bed
 k_e = stagnant effective thermal conductivity of a packed bed
 k_f = thermal conductivity of fluid
 k_s = thermal conductivity of solid
 k_z = axial thermal dispersion conductivity
 Le = Lewis number
 Nu_ξ = local Nusselt number
 n_p = number density of particles
 P = pressure
 P_i = partial pressure at the catalytic surface
 Pe_H = Peclet number for heat
 Pe_M = Peclet number for mass
 Pr = Prandtl number
 Re = Reynolds number
 R_s = rate of consumption of a reactant
 R_{s0} = rate of consumption of a reactant at T_0
 r = radial coordinate
 r_0 = radius of a cylindrical packed column
 S = molar concentration of a reactant
 Sc = Schmidt number
 S_F = molar concentration of a reactant in feed

T = temperature
 T_c = temperature of the core region at the inlet of the reactor
 T_i = temperature at the inlet of the reactor
 T_m = mean fluid temperature
 T_w = wall temperature
 T_0 = inlet temperature of feed
 U = dimensionless axial velocity
 u = axial velocity
 u_m = mean axial velocity
 x = conversion
 $\langle x \rangle$ = mean conversion
 y = quantity defined by $(r_0 - r)/d_p$
 y_F = mole fraction of sulfur dioxide in feed
 z = axial coordinate
 z_I = length of a prereaction zone
 Γ = ratio of the radius of a packed column to the particle diameter
 γ_{dl} = lateral mixing function for heat
 γ_{dM} = lateral mixing function for mass
 δ_d = dimensionless transverse dispersion conductivity for mass
 δ_e = dimensionless effective molecular diffusivity
 ζ = dimensionless distance from the wall
 η = dimensionless radial coordinate
 η_b = Eq. (18)
 θ = dimensionless temperature
 θ_c = dimensionless temperature of the core region at the inlet of the reactor
 θ_i = dimensionless temperature at the inlet of the reactor
 θ_m = dimensionless mixing cup temperature
 θ_w = dimensionless wall temperature
 κ = ratio of thermal conductivity of the solid to that of the fluid
 λ_d = dimensionless thermal dispersion conductivity
 λ_e = dimensionless effective thermal conductivity of a packed bed
 λ_z = dimensionless axial effective thermal conductivity
 μ = viscosity of fluid
 ν = kinematic viscosity of fluid
 ξ = dimensionless axial coordinate
 ξ_I = dimensionless length of the prereaction zone
 ρ = density of fluid
 ρ_s = density of packed sphere
 ϕ = porosity
 ϕ_0 = porosity at the centerline of a reactor

Subscript
 ∞ = quantity at $\phi = 0.39$

Received March 28, 1994; revision received Dec. 5, 1994; accepted for publication Dec. 5, 1994. Copyright © 1995 by K. Kamiuto and S. Saitoh. Published by the American Institute of Aeronautics and Astronautics, Inc., with permission.

*Professor, Department of Production Systems Engineering, Member AIAA.

†Research Associate, Department of Production Systems Engineering.

Superscript

* = dimensionless quantity

Introduction

MATHEMATICAL models for heat and mass transfer within packed bed chemical reactors are indispensable for quantitative prediction of the temperature profiles and conversions in the reactor, and several theoretical models have been proposed in the literature. According to Cheng and Zhu,¹ previous theoretical models may be classified into two groups: 1) the lumped parameter model and 2) the distributed parameter model. The former assumes a plug flow within a reactor and requires constant transverse dispersion coefficient for heat and mass and an apparent wall heat transfer coefficient that must be determined experimentally. The lumped parameter model has been widely utilized for design purposes, but today, it is well-recognized that this model appreciably overpredicts the hot spot temperatures in wall-cooled catalytic reactors,² than are observed. On the other hand, the distributed parameter model allows that local porosity, velocity profile, effective thermal conductivity, effective dispersion coefficients for heat, and mass vary with radial position. Utilizing this kind of model, Ahmed and Fahine³ analyzed simultaneous heat and mass transfer in the sulfur dioxide reactor of Schuler et al.,⁴ and succeeded in predicting the hot spot temperature, the hot spot location, and the mean conversions. However, detailed inspection of their results reveals that the calculated centerline temperature of the reactor does not agree with the experimental data towards the end of the reactor. Moreover, their model does not allow a purely theoretical approach: the experimentally determined velocity profile is utilized and the dispersion coefficients for mass and the effective thermal conductivity are given as an empirical function of radial position.

Recently, the authors⁵ proposed a quasihomogeneous model for analyzing packed bed heat transfer, where the velocity profile was given by solving the momentum equation taking into account the effects of non-Darcy and variable porosity, while the temperature field was determined by solving the energy equation considering the effects of radial thermal dispersion, variable effective thermal conductivity, and thermal radiation.

The purpose of the present study is to extend this model so as to include mass transfer in packed bed catalytic reactors. To this end, a porosity-dependent transverse dispersion coefficient for mass is introduced into the previous model and then, to discuss the adequacy of the model, oxidation of sulfur dioxide to sulfur trioxide over platinum catalysts in the presence of air is analyzed under conditions corresponding to the experiments of Schuler et al.⁴

Governing Equations

The present theoretical model is based on the following assumptions:

- 1) The packed bed reactor is in local thermal equilibrium.
- 2) The wall of the reactor is isothermal and noncatalytic.
- 3) The radial porosity variations are considered. The velocity, the transverse dispersion coefficients for heat and mass, and the effective thermal conductivity are permitted to vary with radial position.
- 4) The fluid is incompressible and the flowfield in the reactor is fully developed at the inlet to the reactor.
- 5) Viscous dissipation and axial conduction terms in the energy equation are neglected.
- 6) Axial diffusion terms in the conservation equations for chemical species are disregarded.
- 7) A correction is made for axial conduction in the inlet region to the reactor.
- 8) Radiation effects are negligible. This assumption is fully justified for packed spheres impregnated with platinum because the surface emissivity of such spheres is sufficiently low.

Under the previously mentioned assumptions, the steady-state governing equations are described as follows:

$$\frac{\partial u}{\partial z} = 0 \quad (1)$$

$$u \frac{\partial S}{\partial z} = \frac{1}{r} \frac{\partial}{\partial r} \left[r(D_e + D_d) \frac{\partial S}{\partial r} \right] - R_s \rho_s (1 - \phi) \quad (2)$$

$$\frac{\mu}{K} u + \rho C u^2 = -\frac{dP}{dz} + \frac{\mu}{\phi} \frac{1}{r} \frac{\partial}{\partial r} \left(r \frac{\partial u}{\partial r} \right) \quad (3)$$

$$\rho C_p u \frac{\partial T}{\partial z} = \frac{1}{r} \frac{\partial}{\partial r} \left[r(k_e + k_d) \frac{\partial T}{\partial r} \right] + R_s \rho_s (1 - \phi)(-H) \quad (4)$$

where K and C represent the permeability and inertial coefficient given by

$$K = d_p^2 \phi^3 / 150(1 - \phi)^2 \quad (5)$$

$$C = 1.75(1 - \phi) / d_p \phi^3 \quad (6)$$

Moreover, D_e and D_d are the effective molecular diffusivity and mass dispersion coefficient of a reactant within a packed bed reactor, while k_e and k_d are the effective thermal conductivity and thermal dispersion conductivity of a packed bed reactor. These quantities will be discussed in the section on the physical properties.

The boundary conditions for Eqs. (2–4) are

$$\begin{aligned} r = 0: \quad & \frac{\partial u}{\partial r} = \frac{\partial T}{\partial r} = \frac{\partial S}{\partial r} = 0 \\ r = r_0: \quad & u = 0, T = T_w \quad \text{and} \quad \frac{\partial S}{\partial r} = 0 \\ z = 0: \quad & T = T_i(r) \quad \text{and} \quad S = S_f \end{aligned} \quad (7)$$

Dimensionless Governing Equations

The following dimensionless quantities are introduced to rewrite the governing equations in the dimensionless form:

$$\begin{aligned} C^* &= \frac{C}{C_z}, \quad Da = \frac{K_z}{r_0^2}, \quad Dam = r_0^2 R_{s0} \rho_s \frac{(1 - \phi_z)}{S_f D_m} \\ E_u &= -\left(\frac{dP}{dx} \right) / \left(\frac{\rho u_m^2}{r_0} \right), \quad Fh = C_z r_0 \\ H^* &= \frac{(-H) S_f}{\rho C_p T_0}, \quad K^* = \frac{K_z}{K}, \quad Le = \frac{\nu k_f}{\mu C_p D_m} \\ Pr &= \frac{\mu C_p}{k_f}, \quad Re = \frac{2u_m r_0}{\nu}, \quad R_s^* = \frac{R_s(1 - \phi)}{R_{s0}(1 - \phi_z)} \\ Sc &= \frac{\nu}{D_m}, \quad U = \frac{u}{u_m}, \quad x = \frac{(S_f - S)}{S_f} \\ \delta_d &= \frac{D_d}{D_m}, \quad \delta_e = \frac{D_e}{D_m}, \quad \Gamma = \frac{r_0}{d_p}, \quad \eta = \frac{r}{r_0} \\ \theta &= \frac{T}{T_0}, \quad \theta_i = \frac{T_i}{T_0}, \quad \theta_w = \frac{T_w}{T_0}, \quad \lambda_d = \frac{k_d}{k_f} \\ \lambda_e &= \frac{k_e}{k_f}, \quad \xi = \left(\frac{x}{2r_0} \right) / RePr \end{aligned} \quad (8)$$

Introducing these dimensionless quantities yields the governing equations of the form:

$$\frac{1}{4} LeU \frac{\partial x}{\partial \xi} = \frac{1}{\eta} \frac{\partial}{\partial \eta} \left[\eta (\delta_c + \delta_d) \frac{\partial x}{\partial \eta} \right] + Dam R_s^* \quad (9)$$

$$\frac{1}{2} EuRe = \frac{K^*}{Da} U + \frac{1}{2} C^* FhReU^2 - \frac{1}{\phi} \frac{1}{\eta} \frac{\partial}{\partial \eta} \left(\eta \frac{\partial U}{\partial \eta} \right) \quad (10)$$

$$\frac{1}{4} U \frac{\partial \theta}{\partial \xi} = \frac{1}{\eta} \frac{\partial}{\partial \eta} \left[\eta (\lambda_c + \lambda_d) \frac{\partial \theta}{\partial \eta} \right] + \left(\frac{H^* Dam}{Le} \right) R_s^* \quad (11)$$

The equation of continuity may be rewritten in the following form:

$$2 \int_0^1 U \eta \, d\eta = 1 \quad (12)$$

The relevant boundary conditions can also be rewritten as

$$\begin{aligned} \eta = 0: \quad & \frac{\partial U}{\partial \eta} = \frac{\partial \theta}{\partial \eta} = \frac{\partial x}{\partial \eta} = 0 \\ \eta = 1: \quad & U = 0, \quad \theta = \theta_w \quad \text{and} \quad \frac{\partial x}{\partial \eta} = 0 \\ \xi = 0: \quad & \theta = \theta_i(\eta) \quad \text{and} \quad x = 0 \end{aligned} \quad (13)$$

Boundary Condition for Temperature at the Inlet of the Reactor

The sulfur dioxide reactor of Schuler et al.,⁴ which is theoretically analyzed here, consisted of a 15.24-cm-length bed packed with alumina catalysts impregnated with platinum, and was preceded by a 10.16-cm-bed of inactive packings. Sulfur dioxide and air entered the prereaction zone at 400°C. The stainless steel walls were cooled at 200°C. The total pressure of the reactor was kept at 1.053 bar during the experiments. The relevant physical model and the coordinate system are shown in Fig. 1.

Because of comparatively small Reynolds number, i.e., $Re = 751.1$, the effects of axial conduction on the temperature profile at the entrance of the reactor are appreciable and should be taken into account. However, the inclusion of axial conduction results in a two-point boundary value problem that greatly increases the complexity of the numerical analysis. To circumvent this complexity and to enjoy the merit of an initial value problem, Ahmed and Fahien³ proposed an approximate method where the effect of axial conduction is considered only in the entrance region by appropriately correcting the inlet thermal boundary condition. In accord with Ahmed and Fahien,³ the prereaction zone is modeled as a region with an isothermal core enclosed by a developing thermal boundary layer. From this model, the temperature profile in the thermal boundary layer ($\eta_b \leq \eta \leq 1$) at the entrance to the reactor is given by

$$\theta_i = a + b\eta^2 + c\eta^4 \quad (14)$$

The coefficients involved in Eq. (14) are determined by the following conditions:

$$\begin{aligned} \eta = 1: \quad & \theta_i = \theta_w \\ \eta = \eta_b: \quad & \theta_i = \theta_c \quad \text{and} \quad \frac{\partial \theta_i}{\partial \eta} = 0 \end{aligned} \quad (15)$$

As a result, Eq. (14) may be rewritten as

$$\begin{aligned} \theta_i = & [\theta_c(1 - 2\eta_b^2) + \theta_w\eta_b^4 + 2\eta_b^2(\theta_c - \theta_w)\eta^2 \\ & - (\theta_c - \theta_w)\eta^4]/(1 - \eta_b^2)^2 \end{aligned} \quad (16)$$

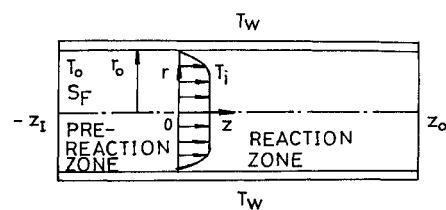


Fig. 1 Physical model and the coordinate system.

To determine a value of η_b involved in this equation, the following condition supported experimentally is utilized:

$$\int_0^1 \theta_i \eta \, d\eta \cong \frac{1}{2} \quad (17)$$

Substituting Eq. (16) into Eq. (17) yields

$$\eta_b = \sqrt{(3 - 2\theta_c - \theta_w)/(\theta_c - \theta_w)} \quad (18)$$

For the core region, the following heat balance holds to be true:

$$\rho c_p u_m \frac{dT_c}{dz} = k_z \frac{d^2 T_c}{dz^2} \quad (19)$$

where k_z represents the effective axial thermal conductivity including the axial dispersion effect and was estimated from the relation obtained by Yagi et al.⁶:

$$\lambda_z = k_z/k_f = \lambda_c + 0.75 Re Pr / 2\Gamma \quad (20)$$

The boundary conditions for Eq. (19) are

$$\begin{aligned} z = -z_i: \quad & T_c = T_o \\ z = 0: \quad & \left. \frac{dT_c}{dz} \right|_{0-} = \left. \frac{dT_c}{dz} \right|_{0+} \end{aligned} \quad (21)$$

Equation (19) can be solved analytically and the resultant inlet temperature may be written in the dimensionless form:

$$\theta_c = 1 + \left[\frac{\lambda_z}{(RePr)^2} \right] \left\{ 1 - \exp \left[-\frac{(RePr)^2 \xi_i}{\lambda_z} \right] \right\} \left. \frac{d\theta_c}{d\xi} \right|_{\xi=0+} \quad (22)$$

As readily seen from Eq. (22), the estimation of θ_c requires a value of $d\theta_c/d\xi|_{\xi=0+}$ to be known. However, this value is not known beforehand, and thus, an iterative procedure is needed: we first assume a tentative value of θ_c and then solve the governing equations for the first several steps. Based on the computational results of the temperature profiles thus obtained, we next evaluate a value of $d\theta_c/d\xi|_{\xi=0+}$. If this value agrees with that estimated from Eq. (22), the first assumed value of θ_c is a true one and, therefore, we can proceed the computation toward the end of the reactor. Otherwise, we must restart on the computation with a different value of θ_c .

Moreover, the axial back-diffusion may affect the conversion profile at the entrance to the reactor, but the results of the general model predictions by Young and Finlayson⁷ and their criterion with respect to axial diffusion show that this effect is negligible and, thus, a correction for axial diffusion is not made in the present study.

Numerical Methods

Young and Finlayson⁷ and Ahmed-Fahien³ applied the collocation method to solve the governing equations for simultaneous heat and mass transfer within the SO_2 catalytic converter reported by Schuler et al.,⁴ but we made use of a finite difference method since the radial variations of porosity, ve-

Table 1 Physical properties and bed characteristics of the sulfur dioxide reactor of Schuler et al.⁴

Quantity	Value
Density of the gas	0.552 kg/m ³
Specific heat of the gas	1.06 kJ/kgK
Thermal conductivity of the gas	0.0457 W/mK
Viscosity of the gas	3.31 × 10 ⁻⁵ kg/ms
Molecular diffusivity of SO ₂ in air	0.122 × 10 ⁻⁴ m ² /s
Mass flow rate	0.475 kg/sm ²
Feed temperature	400°C
Sulfur dioxide in feed	0.066 mole fraction
Wall temperature	200°C
Reactor tube radius	2.62 × 10 ⁻² m
Particle diameter	0.318 × 10 ⁻² m
Density of the catalyst	1708.7 kg/m ³
Thermal conductivity of the catalyst	0.866 W/mK
Length of the prereaction zone	10.16 × 10 ⁻² m
Length of the reactor	15.24 × 10 ⁻² m
Heat of reaction	-9.537 × 10 ⁷ J/kmol

Table 2 Values of the dimensionless parameters utilized for the numerical analyses

Quantity	Value
<i>Dam</i>	748.57
<i>H*</i>	0.301
<i>Le</i>	6.811
<i>Pr</i>	0.721
<i>Sc</i>	4.911
<i>Re</i>	751.1
<i>Γ</i>	8.24
<i>θ_w</i>	0.703

locity, temperature, and conversion are too oscillatory to analytically represent their profiles with several terms of orthogonal functions. The finite difference schemes adopted in this study were the same as described in Ref. 5 and the numerical code was prepared by revising our previous one.⁵ Thus, for finite difference calculations, the dimensionless radius of the reactor was divided into 350 equally spaced increments. The accuracy of the present numerical calculations was checked by comparing the results for the mean conversion $\langle x \rangle$ and mixing cup temperature θ_m at $\xi = 5.09 \times 10^{-3}$ with more accurate results that were obtained by utilizing 2000 divisions for discretizing the energy equation and the conservation equation of the reactant. The comparison showed that the difference between two calculations is quite small: the present results are $\langle x \rangle = 0.3888$ and $\theta_m = 0.8405$, while the more accurate results are $\langle x \rangle = 0.3889$ and $\theta_m = 0.8412$. The parameters for the simulation of the SO₂ reactor of Schuler et al. are summarized in Tables 1 and 2.

Heat Transfer Characteristics and Mean Conversion

The mixing cup temperature is defined by

$$T_m = 2\pi \int_0^{r_0} T(r)u(r)r \frac{dr}{\pi r_0^2 u_m} \quad (23)$$

and may be rewritten in the dimensionless form

$$\theta_m = 2 \int_0^1 U(\eta)\theta(\eta)\eta \, d\eta \quad (24)$$

Similarly, the mean conversion is given by

$$\begin{aligned} \langle x \rangle &= 2\pi \int_0^{r_0} x(r)u(r) \frac{r \, dr}{\pi r_0^2 u_m} \\ &= 2 \int_0^1 x(\eta)U(\eta)\eta \, d\eta \end{aligned} \quad (25)$$

The local Nusselt number is defined by

$$Nu_\xi = \frac{2r_0 h_x}{k_f} = \frac{2 \left. \frac{\partial \theta}{\partial \eta} \right|_{\eta=1}}{\theta_w - \theta_m} \quad (26)$$

Physical Properties

The effective thermal conductivity appearing in Eq. (4) was evaluated from Bruggeman's theory. For a gas-solid system, the dimensionless effective thermal conductivity may be written as

$$\lambda_e = k_e/k_f = (\kappa - 1)\kappa^{1/3} \phi [\sqrt[3]{(-1 + A)/2} - \sqrt[3]{(1 + A)/2}] + \kappa \quad (27)$$

where $A = 1 + (4/27)\phi^3(\kappa - 1)^3/\kappa^2$ and $\kappa = k_s/k_f$. The adequacy of Bruggeman's theory has fully been examined in Ref. 8.

The thermal dispersion conductivity k_d represents a degree of thermal transport due to the lateral mixing of local fluid streams within a packed bed and the dimensionless thermal dispersion conductivity is generally represented by

$$\lambda_d = k_d/k_f = \gamma_{dl} Pr Re U(\eta)/2\Gamma \quad (28)$$

where γ_{dl} denotes a lateral mixing function for heat (or a reciprocal of Peclet number for heat dispersion, Pe_H). γ_{dl} depends on a local porosity and is represented in the following form:

$$\gamma_{dl}(\phi) = a(1 - \phi)^b \quad (29)$$

The values of a and b are determined so as to reproduce Kunii's theoretical estimate for the wall region⁹ and the experimental data¹⁰ for the packed bed with $\Gamma \rightarrow \infty$, i.e., $\gamma_{dl}(0.7) = 0.02$ and $\gamma_{dl}(0.356) = 0.1232$. The determined values are 0.3519 for a and 2.3819 for b .

The effective molecular diffusivity D_e in a packed bed reactor was evaluated from

$$D_e = \phi D_m \quad (30)$$

where D_m is the molecular diffusivity of a reactant in air.

The mass dispersion coefficient D_d denotes a degree of mass diffusion due to the lateral mixing of local fluid stream within a reactor and was given by

$$\delta_d = D_d/D_m = \gamma_{dM} Sc Re U(\eta)/2\Gamma \quad (31)$$

where γ_{dM} is a lateral mixing function for mass (or a reciprocal of Peclet number for mass dispersion, Pe_M). Here, we assumed that $Pe_M = K' Pe_H$, since mass and heat dispersions occur due to the same mechanism. A value of K' was determined utilizing experimental values^{10,11} of Pe_H and Pe_M for $\phi = 0.356$ corresponding to $\Gamma \rightarrow \infty$, i.e., $Pe_H = 8.1157$ and $Pe_M = 8$, and was found to be 0.9857. As a result, the lateral mixing function for mass becomes

$$\gamma_{dM} = 0.3569(1 - \phi)^{2.3819} \quad (32)$$

The local porosity distribution function was given by the Ridgeway-Tarback distribution,¹² which is written as follows:

For $0 \leq \zeta \leq 0.6$

$$\phi(\zeta) = 1 - 3.10036\zeta + 3.70243\zeta^2 - 1.24612\zeta^3 \quad (33)$$

For $0.6 < \zeta \leq \Gamma$ (≥ 5)

$$\phi(\zeta) = -0.1865 \exp(-0.22\zeta^{1.5}) \cos(7.66\zeta_1) + 0.39$$

where $\zeta_1 = \zeta - 0.6$, $\zeta = y/d_p$, and y represents the distance from the wall.

The rate expression for oxidization of sulfur dioxide to sulfur trioxide over platinum catalysts in the presence of air may be written in the following form¹³:

$$R_s = k(P_{O_2}^{1/2}P_{SO_2} - P_{SO_3}/K_0)/[1 + (K_1P_{O_2})^{1/2} + K_2P_{SO_3}]^2 \quad (34)$$

where P_i denotes partial pressure of i at the catalyst surface, k the specific rate constant, K_1 the adsorption equilibrium constant for oxygen, K_2 the adsorption equilibrium constant for SO_3 , K_0 the equilibrium constant, and T the catalyst temperature (K). These quantities are represented in the following form:

$$\begin{aligned} P_{O_2} &= 0.21(1 - y_F) - 0.5y_Fx \\ P_{SO_2} &= y_F(1 - x) \\ P_{SO_3} &= y_Fx \\ k &= A_1 \exp(B_1/T) \\ \sqrt{K_1} &= A_2 \exp(B_2/T) \\ K_2 &= A_3 \exp(B_3/T) \end{aligned} \quad (35)$$

where y_F denotes the mole fraction of sulfur dioxide in feed ($=0.066$). Values of A_1 , A_2 , A_3 , B_1 , B_2 , and B_3 were determined so as to reproduce the experimental data of reaction rate described in Ref. 14. The obtained results are $A_1 = 17.25$ (kmol/s/kg-catalyst), $A_2 = \exp(-31.43)$, $A_3 = \exp(-0.5468)$, $B_1 = -6904.4$, $B_2 = 19,746.5$, and $B_3 = 2691.9$. The equilibrium constant was taken from Ref. 13 and was given by

$$K_0 = \exp(11,572.2/T - 10.05) \quad (36)$$

As seen from Fig. 2, the agreement between the present correlation and the experimental data is excellent.

Results and Discussion

The calculated velocity profile is shown in Fig. 3, where the experimental results obtained by Morales et al.¹⁵ are denoted by the symbols. The velocity profile oscillates periodically in accord with the radial porosity variations. There exists a discrepancy between the theoretical result and the experimental ones, but it should be noted that the indicated experimental data were taken at the distance of $\frac{3}{8}$ in. above the top of the packing and, thus, expected oscillatory velocity variations were appreciably smoothed out.

Figure 4 shows a comparison between the theoretically calculated temperature profiles and the experimental ones. The calculated temperature profiles are characterized by the steep temperature gradient at the cold wall, which was caused by

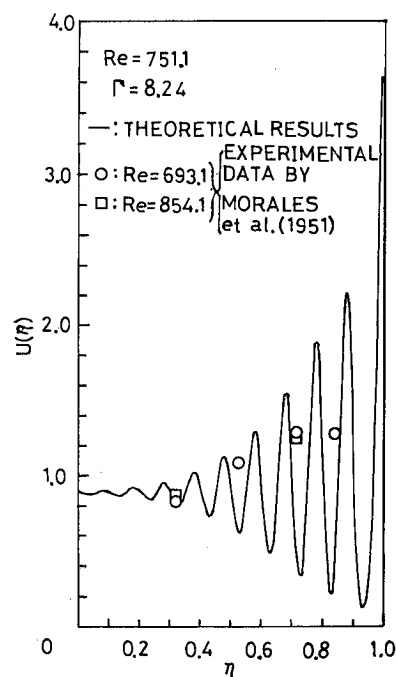


Fig. 3 Radial velocity profile within the sulfur dioxide reactor.

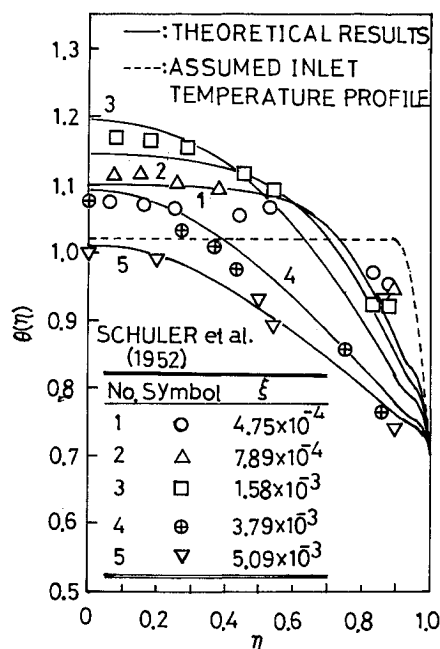


Fig. 4 Radial temperature profiles within the sulfur dioxide reactor.

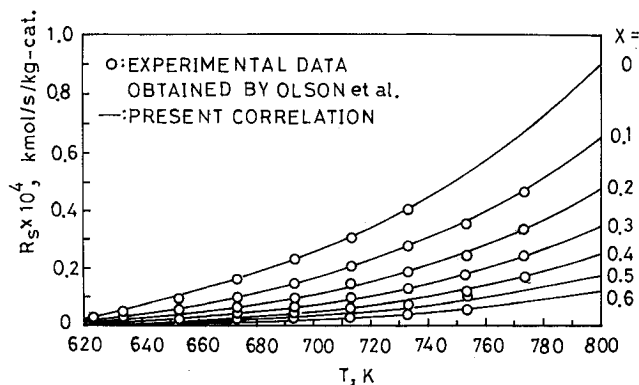


Fig. 2 Rate of oxidation of SO_2 over alumina catalysts impregnated with platinum.

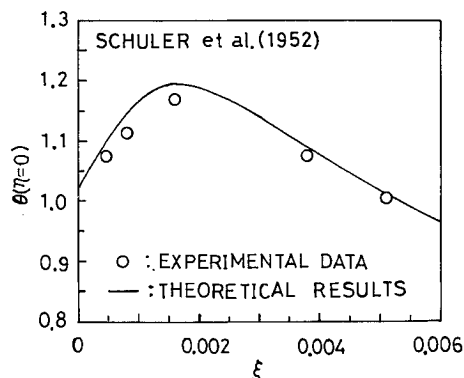


Fig. 5 Axial variations in the centerline temperature of the sulfur dioxide reactor.

the effects of a reduction in the thermal dispersion and wall channeling. Moreover, it is found that the predicted temperature profiles are wavy. This stems from the fact that the local effective thermal conductivity affecting the local temperature profiles was allowed to vary in accord with the local porosity distribution. There exists little discrepancy between theory and experiment in the inlet region of the reactor: the predicted results are slightly higher than the experimental data in the central core of the reactor. Despite this discrepancy, the agreement between them is acceptable in view of uncertainty in the experiment.

The comparison between the predicted centerline temperature and the experimental one is made in Fig. 5. The location of the hot spot temperature is well-predicted, while the predicted temperature is a little higher than the experimental result.

The calculated conversion profiles are shown in Fig. 6. The obtained profiles oscillate periodically in accord with the local porosity variations and the conversion gradient at the cold boundary becomes zero because the wall was assumed to be noncatalytic.

The axial variations in the mean conversion are shown in Fig. 7. The theoretical predictions agree excellently with the experimental data, and this supports the adequacy of the proposed porosity-dependent mass dispersion coefficient.

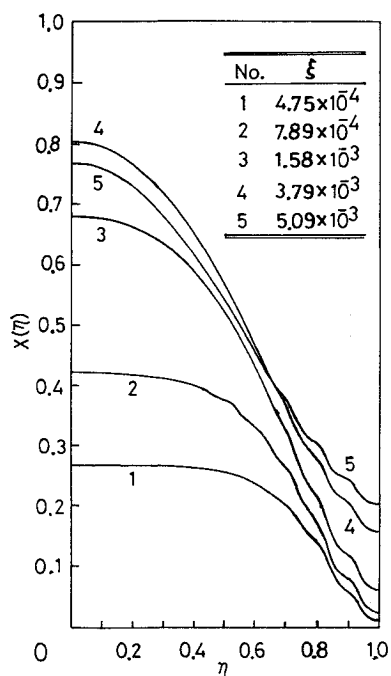


Fig. 6 Radial conversion profiles within the sulfur dioxide reactor.

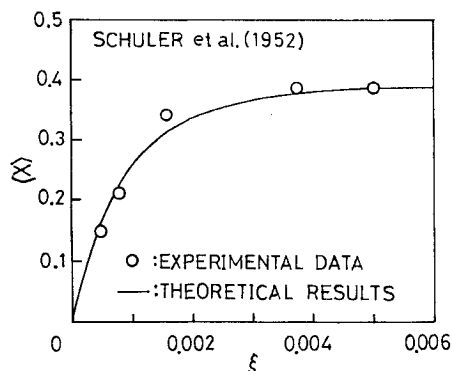


Fig. 7 Relations between the mean conversion and the dimensionless axial distance for the sulfur dioxide reactor.

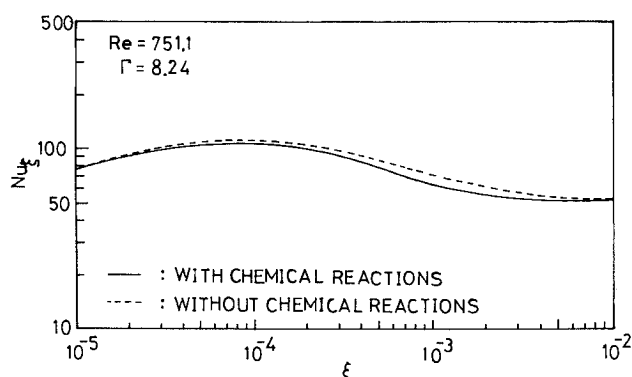


Fig. 8 Relations between the local Nusselt numbers and the axial distance for the sulfur dioxide reactor.

Variations of the local Nusselt number against the dimensionless axial distance are shown in Fig. 8, where the computed result for pure convection is denoted by the broken line, while the case considering chemical reaction is represented by the solid line. As seen from this figure, only a little difference exists between them: the Nusselt number for the chemically reacting flow is slightly lower than that for pure convection, since, for the former case, the temperature gradient at the wall becomes dull due to the amount of heat released by the chemical reaction.

Conclusions

The quasihomogeneous model for simultaneous heat and mass transfer in catalytic packed beds was described. The Darcy-Brinkman-Ergun model was utilized as the momentum equation, with the radial porosity variations considered. The energy equation included the effects of variable stagnant effective thermal conductivity and porosity-dependent transverse thermal dispersion. In addition, the effects of porosity-dependent transverse mass dispersion were taken into account in the equation of continuity for chemical species. Based on the proposed model, oxidation processes of sulfur dioxide to sulfur trioxide in a cylindrical catalytic reactor were analyzed under conditions as reported by Schuler et al.⁴ The theoretical results for the temperature profiles and mean conversions agreed satisfactorily with the experimental data, and this confirms the adequacy of the present model involving no adjustable parameters.

References

- ¹Cheng, P., and Zhu, H., "Effects of Radial Thermal Dispersion on Fully-Developed Forced Convection in Cylindrical Packed Tubes," *International Journal of Heat and Mass Transfer*, Vol. 30, No. 11, 1987, pp. 2373-2383.
- ²Paterson, W. R., and Carberry, J. J., "Fixed Bed Catalytic Reactor Modelling," *Chemical Engineering Science*, Vol. 38, No. 1, 1983, pp. 175-180.
- ³Ahmed, M., and Fahien, R. W., "Tubular Reactor Design-I," *Chemical Engineering Science*, Vol. 35, 1980, pp. 889-895.
- ⁴Schuler, R. W., Stallings, V. P., and Smith, J. M., "Heat and Mass Transfer in Fixed-Bed Reactors," *Chemical Engineering Progress Symposium Series No. 4*, Vol. 48, 1952, pp. 19-30.
- ⁵Kamiuto, K., and Saitoh, S., "Combined Forced-Convection and Correlated-Radiation Heat Transfer in Cylindrical Packed Beds," *Journal of Thermophysics and Heat Transfer*, Vol. 8, No. 1, 1994, pp. 119-124.
- ⁶Yagi, S., Kunii, D., and Wakao, N., "Studies on Effective Thermal Conductivities in Packed Beds," *AIChE Journal*, Vol. 6, No. 4, 1960, pp. 543-546.
- ⁷Young, L. C., and Finlayson, B. A., "Axial Dispersion in Non-isothermal Packed Bed Chemical Reactors," *Industrial and Engineering Chemistry Fundamentals*, Vol. 12, No. 4, 1973, pp. 412-422.
- ⁸Kamiuto, K., "Examination of Bruggeman's Theory for Effective Thermal Conductivities of Packed Beds," *Journal of Nuclear Science and Technology*, Vol. 27, No. 5, 1990, pp. 473-476.

⁹Kunii, D., *Thermal Unit Operations*, Vol. 1, Maruzen, Tokyo, 1976, p. 149.

¹⁰Yagi, S., Kunii, D., and Wakao, N., "Radially Effective Thermal Conductivities in Packed Beds," *International Developments in Heat Transfer*, Pt. III, American Society of Mechanical Engineers, New York, 1961, pp. 742-749.

¹¹Fahien, R. W., and Smith, J. M., "Mass Transfer in Packed Beds," *AIChE Journal*, Vol. 1, No. 1, 1955, pp. 28-37.

¹²Ridgway, K., and Tarbuck, K. J., "Radial Voidage Variations in Randomly-Packed Beds of Spheres of Different Sizes," *Journal of*

Pharmacy and Pharmacology, Vol. 18, Supplement, 1966, pp. 168S-175S.

¹³Uyehara, O. A., and Watson, K. M., "Oxidation of Sulfur Dioxide," *Industrial and Engineering Chemistry*, Vol. 35, No. 5, 1943, pp. 541-545.

¹⁴Smith, J. M., *Chemical Engineering Kinetics*, 2nd ed., McGraw-Hill, New York, 1970, p. 533.

¹⁵Morales, M., Spinn, W. O., and Smith, J. M., "Velocities and Effective Thermal Conductivities in Packed Beds," *Industrial and Engineering Chemistry*, Vol. 43, No. 1, 1951, pp. 225-232.